

## A New Ceria-Zirconia Mixed Oxide Phase Based on Pyrochlore

Toshiyuki Masui, Tetsuya Ozaki, Gin-ya Adachi,\* Zhenchuan Kang,<sup>†</sup> and LeRoy Eyring<sup>†</sup>

*Department of Applied Chemistry, Faculty of Engineering, Osaka University, 2-1 Yamadaoka, Suita, Osaka 565-0871*

*<sup>†</sup>Department of Chemistry and Biochemistry, Arizona State University, Tempe, AZ 85287-1604, U.S.A.*

(Received May 1, 2000; CL-000415)

A new oxygen-rich ceria-zirconia pyrochlore phase has been produced by thermal decomposition of cerium-zirconyl oxalate in an argon flow and subsequent oxidation at 673 K for 2 h; it has been identified with high resolution electron microscopy.

Ceria-zirconia solid solutions have been recognized as a key material of the automotive exhaust catalysts since it can release and uptake oxygen owing to the rapid reversible oxidation states of cerium between  $\text{Ce}^{3+}$  and  $\text{Ce}^{4+}$ .<sup>1,2</sup> This oxygen storage property is essential in the automotive exhaust converters to adjust the air to fuel ratio to the stoichiometric value ( $\approx 14.6$ ) and to establish high conversion efficiency.<sup>3</sup> Therefore, the textural and structural characterization of the ceria-zirconia mixed oxides have been investigated.<sup>4</sup> Recently, it has been reported that the reduction behavior of the ceria-zirconia solid solutions was strongly promoted by several preparation processes via pyrochlore phase.<sup>5,6</sup> We also have found that a  $\text{CeO}_2$ - $\text{ZrO}_2$  solid solution prepared by thermal decomposition of cerium-zirconyl oxalate in an inert gas and subsequent mild temperature oxidation had high oxygen storage capacity.<sup>7</sup> Although a few oxygen-rich pyrochlore phases have been found by powder X-ray and neutron diffraction,<sup>6,8</sup> the direct observation of the oxygen-rich pyrochlore phase using high resolution electron microscopy (HREM) has, as far as we aware, not been reported. In this paper we applied an HREM technique to attain the direct observation of a new oxygen-rich ceria-zirconia pyrochlore phase  $\text{Ce}_2\text{Zr}_2\text{O}_{7.5}$ .

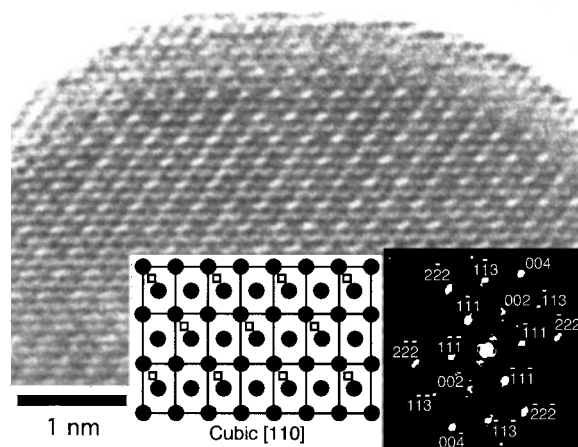
The ceria-zirconia mixed oxide was prepared by thermal decomposition of coprecipitated cerium-zirconyl mixed oxalate according to a procedure published previously.<sup>7</sup> Briefly, the precipitate of cerium zirconyl oxalate  $\text{Ce}_2(\text{ZrO})_2(\text{C}_2\text{O}_4)_{5-n}\text{H}_2\text{O}$  was formed by adding a mixture of  $1.0 \text{ mol}\cdot\text{dm}^{-3}$  aqueous solutions of cerium nitrate and zirconyl nitrate with Ce/Zr ratio of 1/1 to  $0.5 \text{ mol}\cdot\text{dm}^{-3}$  oxalic acid solution and subsequently adjusting the pH value of the solution to 2 with ammonium hydroxide. The precipitate was washed with deionized water several times, dried at 353 K overnight. The powder obtained was heated in an argon flow at 1273 K for 5 h and subsequently oxidized in air at 673 K for 2 h.

The HREM images were recorded using a JEOL4000-EX microscope operating at 400 kV. Samples were prepared by dipping a 3-mm holey carbon copper grid into an ultrasonic dispersion of the oxide powder in ethanol. Selected area electron diffraction (SAED) patterns and HREM micrographs were digitized and analyzed using the DigitalMicrograph<sup>TM</sup> (Gatan Inc.) software package. Digital diffraction patterns (DDPs) were calculated using this software as the Fourier transform of the two dimensional intensity distributions in the images.

The average composition of the samples in a macro scale

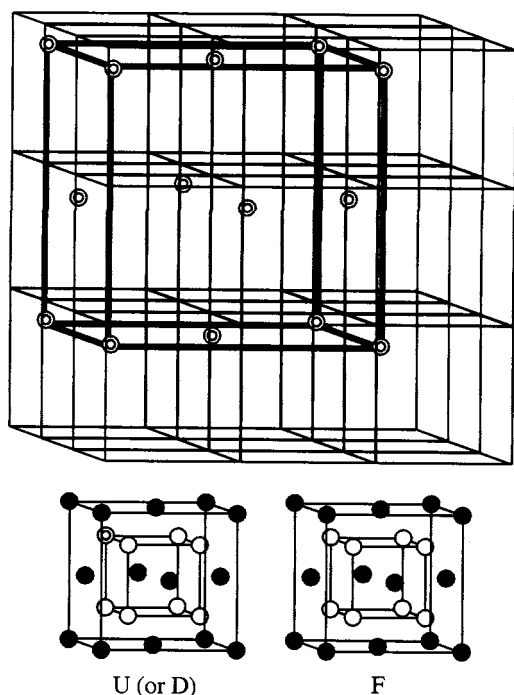
was identified using an X-ray fluorescence spectrometer (Rigaku System 3270A) to be  $\text{Ce}_{0.45}\text{Zr}_{0.55}\text{O}_2$ . X-Ray powder diffraction pattern using  $\text{CuK}\alpha$  radiation (MAC Science M18XHF-SHA) showed a single phase attributed to an apparent cubic fluorite structure, but the width of each peak was relatively broad. The oxygen storage capacity and specific surface area measured using a thermal conductivity detector (Shimadzu GC-8A and Micromeritics FlowSorb II 2300) were  $7.95 \times 10^{-4} \text{ mol}\cdot\text{g}^{-1}$  and  $4 \text{ m}^2\cdot\text{g}^{-1}$ , respectively.

Figure 1 shows a typical HREM image of the sample with its DDP inset. The micrograph contained clear evidence for crystals with a cubic phase which showed double spacing. The clear double space lattice image in this figure most likely arises from an ordered arrangement of oxygen vacancies. The crystal also presents a fluorite-related cubic-type DDP which corresponds to the zone axes [110], and the DDP indicates the geometry and superlattice features.



**Figure 1.** HREM image of the ceria-zirconia mixed oxide sample showing part of the  $\text{Ce}_2\text{Zr}_2\text{O}_{7.5}$  crystal, corresponding DDP and a model of the HREM image. The DDP can be indexed to the cubic structure with superstructure viewed along the [110] zone axis. Filled dots and open squares represent metal ions and oxygen vacancies, respectively.

Figure 2 shows a model of the structure derived from the micrograph in Figure 1. The array of the fluorite-related superstructure is considered as face shared modules of the fluorite-type representing all allowed vacancy configurations.<sup>9</sup> According to the matching procedure between experimental and deployment of the vacant oxygen sites, the superstructure consists of only the two type modules F and U (or D) and these modules are arranged one after the other in three dimensions, where the F has no vacancies and the U (or D) contains a vacant



**Figure 2.** A model of the structure of  $\text{Ce}_2\text{Zr}_2\text{O}_{7.5}$  phase derived from the micrograph in Figure 1. Two fluorite-based modules that have one or no anion deficiency arrange one after the other in three dimensions. Oxygen vacancies which are represented by double circles form the face-centered cubic arrangement in a double-spacing unit.

oxygen site in the top half (or in the bottom half). The composition of this phase corresponds to  $\text{Ce}_2\text{Zr}_2\text{O}_{7.5}$ . This new phase has not been reported in previous references and the present study elucidates its existence directly for the first time. It is not clear whether the cation arrangement is ordered or not, but probably the ordering level of the cations in this phase will be low, taking the results of the oxygen-rich pyrochlore phase prepared using hydrogen reduction into consideration.<sup>6</sup>

The production of the oxygen-rich pyrochlore phase is also supported by the results of the Raman spectra previously reported.<sup>7</sup> Raman scattering is generally detectable within a depth of 10–100 nm from the surface of a sample. The sample showed three peaks centered at 304, 470, and 578  $\text{cm}^{-1}$  attributed to the pyrochlore-based structure as well as the other three tetragonal  $E_g$  bands centered at 272, 446, and 611  $\text{cm}^{-1}$ . Indeed, some particles which are attributed to the tetragonal structure were also observed in several HREM images of this sample.

Experimental SAED patterns of the aggregated powder were analyzed and the d-spacing values were calculated from the positions of the diffraction rings and spots. The diffraction rings from the fluorite cubic structure were dominantly observed and they corresponded to interplaner spacings of 0.30<sub>4</sub>, 0.26<sub>3</sub>, and 0.18<sub>6</sub> nm. The other spots were from tetragonal and double-spacing cubic phases. The isolated spots at 0.21<sub>2</sub>, 0.23<sub>3</sub>, 0.37<sub>0</sub> and 0.52<sub>0</sub> nm were for the tetragonal phase, and the other ones at 0.60<sub>8</sub> nm were for the double-spacing cubic phase. The Raman, HREM and SAED results mentioned above mean that the sample is a mixture of the cubic and tetragonal phases on a very fine scale, since the phase separation could not be observed in the XRD measurement.

In the present study, finely divided carbon particles are uniformly formed in the starting ceria-zirconia mixed oxide because the sample is prepared by the decomposition of cerium-zirconyl oxalate in an inert gas flow. These fine carbon particles work as a reductant during the decomposition process. Since the Gibbs free energy at 1273 K for the reduction of  $\text{CeO}_2$  to  $\text{Ce}_2\text{O}_3$  by carbon was lower than that for the reduction by hydrogen or carbon monoxide,<sup>10</sup> thermal decomposition of the oxalate in an argon atmosphere would more effectively produce the pyrochlore  $\text{Ce}_2\text{Zr}_2\text{O}_7$  solid solution than the other reduction process. During the oxidation of the pyrochlore phase, the most of excessive fine carbon particles were eliminated by the subsequent calcination at 673 K, since hydrocarbons, CO, and  $\text{CO}_2$  evolution could not be detected in the measurement of oxygen storage capacity. In some previous references,<sup>6,8</sup> a few oxygen rich pyrochlore phases such as  $\text{Ce}_2\text{Zr}_2\text{O}_8$  and  $\text{Ce}_2\text{Zr}_2\text{O}_{7.97}$  were prepared via hydrogen reduction and subsequent reoxidation process between 773 and 873 K. In the sample of this study, the intercalation of the oxygen anions into the lattice would not be complete especially in the surface region of the aggregated powders because the oxidation temperature was as low as 673 K. It is suggested, therefore, that an incompletely oxidized pyrochlore phase  $\text{Ce}_2\text{Zr}_2\text{O}_{7.5}$  has been produced and this new phase would be responsible for high oxygen storage capacity of our sample.

This work was supported by Grant-in-Aid for Scientific Researches (B) No. 11450335 from the Japan Society for the Promotion of Science (JSPS). Experimental HREM images were obtained at Arizona State University. Arizona State University provided the salary for Z.C.K.

#### References and Notes

- 1 J. Kaspar, P. Fornasiero, and M. Graziani, *Catal. Today*, **50**, 285 (1999).
- 2 A. Trovarelli, C. de Leitenburg, and G. Delcetti, *CHEMTECH*, **27**, 32 (1997).
- 3 K. C. Taylor, in "Catalysis—Science and Technology," ed by J. R. Anderson and M. Boudert, Springer-Verlag, Berlin, (1984), Chap. 2.
- 4 G. Colón, M. Pijolat, F. Valdivieso, H. Vidal, J. Kaspar, E. Finocchio, M. Daturi, C. Binet, J. C. Lavalley, R. T. Baker, and S. Bernal, *J. Chem. Soc., Faraday Trans.*, **94**, 3717 (1998).
- 5 P. Fornasiero, G. Balducci, R. Di Monte, J. Kaspar, V. Sergo, G. Gubitosa, A. Ferrero, and M. Graziani, *J. Catal.*, **164**, 173 (1996).
- 6 S. Otsuka-Yao, H. Morikawa, N. Izu, and K. Okuda, *J. Japan Inst. Metals*, **59**, 1237 (1995); S. Otsuka-Yao-Matsuo, T. Omata, N. Izu, and H. Kishimoto, *J. Solid State Chem.*, **138**, 47 (1998); N. Izu, T. Omata, and S. Otsuka-Yao-Matsuo, *J. Alloys Compds.*, **270**, 107 (1998); T. Omata, H. Kishimoto, S. Otsuka-Yao-Matsuo, N. Ohtori, and N. Umetsaki, *J. Solid State Chem.*, **147**, 573 (1999).
- 7 T. Masui, Y. Peng, K. Machida, and G. Adachi, *Chem. Mater.*, **10**, 4005 (1998); T. Ozaki, T. Masui, K. Machida, T. Sakata, H. Mori, and G. Adachi, *Chem. Mater.*, **12**, 643 (2000).
- 8 J. B. Thomson, A. R. Armstrong, and P. G. Bruce, *J. Am. Chem. Soc.*, **118**, 11129 (1996); J. B. Thomson, A. R. Armstrong, and P. G. Bruce, *J. Solid State Chem.*, **148**, 56 (1999).
- 9 Z. C. Kang and L. Eyring, *Aust. J. Chem.*, **49**, 981 (1997); Z. C. Kang and L. Eyring, *J. Alloys Compd.*, **249**, 206 (1997); Z. C. Kang, J. Zhang, and L. Eyring, *Z. Anorg. Allg. Chem.*, **622**, 465 (1996).
- 10 Gmelin Handbuch der Anorganischen Chemie, System Nr. 39, Sc, Y, La und Lanthanide - Seltenerdelemente, Teil C1, Hydride; Oxide, Springer-Verlag, Berlin, (1974), p. 256.